Consensus statement for stability assessment and reporting for perovskite photovoltaics based on ISOS procedures

Khenkin, Mark V. ; Katz, Eugene A. ; Abate, Antonio ; Bardizza, Giorgio ; Berry, Joseph J. ; Brabec, Christoph J.; Brunetti, Francesca ; Bulović, Vladimir ; Burlingame, Quinn ; Di Carlo, Aldo ; Cheacharoen, Rongrong; Cheng, Yi-Bing ; Colsmann, Alexander ; Cros, Stephane ; Domanski, Konrad ; Dusza, Michał; Fell, Christopher J. ; Forrest, Stephen R. ; Galagan, Yulia ; Di Girolamo, Diego ; Grätzel, Michael ; Hagfeldt, Anders ; von Hauff, Elizabeth ; Hoppe, Harald ; Kettle, Jeffrey; Köbler, Hans; Leite, Marina S. ; Liu, Shengzhong (Frank) ; Loo, Yueh-Lin ; Luther, Joey M. ; Ma, Chang-Qi; Madsen, Morten ; Manceau, Matthieu ; Matheron, Muriel ; McGehee, Michael ; Meitzner, Rico ; Nazeeruddin, Mohammad Khaja ; Nogueira, Ana Flavia ; Odabaşı, Çağla ; Osherov, Anna; Park, Nam-Gyu ; Reese, Matthew O. ; De Rossi, Francesca ; Saliba, Michael ; Schubert, Ulrich S.; Snaith, Henry J. ; Stranks, Samuel D. ; Tress, Wolfgang ; Troshin, Pavel A. ; Turkovic, Vida ; Veenstra, Sjoerd ; Visoly-Fisher, Iris ; Walsh, Aron ; Watson, Trystan ; Xie, Haibing ; Yıldırım, Ramazan ; Zakeeruddin, Shaik Mohammed ; Zhu, Kai ; Lira-Cantu, Monica

Nature energy

DOI:
10.1038/s41560-019-0529-5

Published: 01/01/2020

Peer reviewed version

Consensus on ISOS Protocols for Stability Assessment and Reporting for Perovskite Photovoltaics

Mark V. Khenkin[1], Eugene A. Katz[1,2,*], Antonio Abate[3], Giorgio Bardizza[4], Joseph J. Berry[5], Christoph J. Brabec[6,7], Francesca Brunetti[8], Vladimir Bulović[9], Quinn Burlingame[10], Aldo Di Carlo[8], Rongrong Cheacharoen[11], Yi-Bing Cheng[12], Alexander Colsmann[13], Stephane Cros[14], Konrad Domanski[15], Michał Dusza[16], Christopher J. Fell[17], Stephen R. Forrest[18,19,20], Yulia Galagan[21], Diego Di Girolamo[8,22], Michael Grätzel[23], Anders Hagfeldt[24], Elizabeth von Hauff[25], Harald Hoppe[26], Jeff Kettle[27], Hans Köbler[3], Marina S. Leite[28], Shengzhong (Frank) Liu[29,30], Yueh-Lin Loo[10,31], Joey M. Luther[5], Chang-Qi Ma[32], Morten Madsen[33], Matthieu Manceau[14], Muriel Matheron[14], Michael McGehee[5,34], Rico Meitzner[26], Mohammad Khaja Nazeeruddin[35], Ana Flavia Nogueira[36], Çağla Odabaşı[37], Anna Osherov[9], Nam-Gyu Park[38], Matthew O. Reese[5], Francesca De Rossi[8,39], Michael Saliba[40], Ulrich S. Schubert[25,41], Henry J. Snaith[42], Samuel D. Stranks[43], Wolfgang Tress[20,23], Pavel A. Troshin[44,45], Vida Turkovic[33], Sjoerd Veenstra[21], Iris Visoly-Fisher[1,2], Aron Walsh[46,47], Trystan Watson[39], Haibing Xie[48], Ramazan Yıldırım[37], Shaik Mohammed Zakeeruddin[23], Kai Zhu[5] and Monica Lira-Cantu[48,*]

[*]Corresponding authors, e-mail: keugene@bgu.ac.il, monica.lira@icn2.cat

[1]Department of Solar Energy and Environmental Physics, Swiss Inst. for Dryland Environmental and Energy Research, J. Blaustein Institutes for Desert Research, Ben-Gurion University of the Negev, Midreshet Ben-Gurion 8499000, Israel.

[2]Ilse Katz Institute for Nanoscale Science and Technology, Ben-Gurion University of the Negev, Be'er-Sheva 8410501, Israel.

[3] Helmholtz-Zentrum Berlin für Materialien und Energie GmbH, Berlin, Germany.

[4] European Commission, Joint Research Centre (JRC), Ispra (VA), Italy.

[5] National Renewable Energy Laboratory, Golden, Colorado 80401, United States.

[6] Department of Materials Science and Engineering, Friedrich Alexander University Erlangen Nürnberg, Germany.

[7] Helmholtz Institute Erlangen-Nürnberg (HI-ErN), Forschungszentrum Jülich (FZJ), Immerwahrstrasse 2, D-91058 Erlangen, Germany.

[8] CHOSE (Centre for Hybrid and Organic Solar Energy), Department of Electronic Engineering, University of Rome Tor Vergata, via del Politecnico 1, 00133 Rome, Italy.

[9]Department of Electrical Engineering and Computer Science, Massachusetts Institute of Technology Cambridge, MA 02139, USA

[10] Department of Chemical and Biological Engineering, Princeton University, Princeton, New Jersey 08544, USA.

[11] Metallurgy and Materials Science Research Institute, Chulalongkorn University, Bangkok 10330, Thailand.

[12] State Key Laboratory of Advanced Technology for Materials Synthesis and Processing, Wuhan University of Technology, Wuhan 430070, China.

[13] Light Technology Institute, Karlsruhe Institute of Technology (KIT), Engesserstrasse 13, 76131 Karlsruhe, Germany.

[14] Univ. Grenoble Alpes, CEA, LITEN, INES, 73375 Le Bourget du Lac, France.

[15] Fluxim AG, Katharina-Sulzer Platz 2, 8400 Winterthur, Switzerland.

[16] Saule Technologies, Wroclaw Technology Park, Dunska 11, Sigma Building, 54-427 Wroclaw, Poland.

[17] CSIRO Energy, Mayfield West, NSW, 2304 Australia.

[18] Department of Electrical Engineering and Computer Science, University of Michigan, Ann Arbor, MI, 48109, USA

[19] Department of Physics, University of Michigan, Ann Arbor, MI, 48109, USA

[20] Department of Materials Science and Engineering, University of Michigan, Ann Arbor, MI, 48109, USA

[21] TNO - Solliance, High Tech Campus 21, 5656 AE, Eindhoven, The Netherlands.

[22] Department of Chemistry, University of Rome La Sapienza, pzz. le Aldo Moro 5, 00185, Rome, Italy.

[23] Laboratory for Photonics and Interfaces, Institute of Chemical Sciences and Engineering, École Polytechnique Fédérale de Lausanne, Lausanne, Switzerland.

[24] Laboratory of Photomolecular Science, Institute of Chemical Sciences and Engineering, École Polytechnique Fédérale de Lausanne, Lausanne, Switzerland.

[25] Department of Physics and Astronomy, Vrije Universiteit Amsterdam, De Boelelaan, 1081 HV Amsterdam, The Netherlands.

[26] Center for Energy and Environmental Chemistry Jena (CEEC Jena), Friedrich Schiller University Jena, Philosophenweg 7a, 07743 Jena, Germany.

[27] School of Electronic Engineering, Bangor University, Dean Street, Bangor, Gwynedd, Wales LL57 1UT, UK.

[28] Department of Materials Science and Engineering, Institute for Research in Electronics and Applied Physics, University of Maryland, 2123 Chemical and Nuclear Engineering Building, College Park, MD 20742-2115, USA.

[29] Dalian National Laboratory for Clean Energy/Dalian Institute of Chemical Physics, Chinese Academy of Sciences, Dalian 116023, Liaoning, Shaanxi, China.

[30] Key Laboratory for Advanced Energy Devices; Shaanxi Engineering Lab for Advanced Energy Technology; Institute for Advanced Energy Materials; School of Materials Science and Engineering, Shaanxi Normal University, Xi'an 710119, Shaanxi, China.

[31] Andlinger Center for Energy and the Environment, Princeton University, Princeton, New Jersey 08544, USA.

[32] Printable Electronics Research Center, Suzhou Institute of Nano-Tech and Nano-Bionics, Chinese Academy of Sciences (CAS), Suzhou, China.

[33] SDU NanoSYD, Mads Clausen Institute, University of Southern Denmark, Alsion 2, DK-6400 Sønderborg, Denmark.

[34] University of Colorado Boulder, Boulder, Colorado 80309, USA.

[35] Group for Molecular Engineering of Functional Materials, Institute of Chemical Sciences and Engineering, École Polytechnique Fédérale de Lausanne, CH-1951, Sion, Switzerland.

[36] Laboratório de Nanotecnologia e Energia Solar, Chemistry Institute, University of Campinas – UNICAMP, PO Box 6154, 13083-970, Campinas, São Paulo, Brazil.

[37] Department of Chemical Engineering, Boğaziçi University, 34342, Bebek, Istanbul, Turkey.

[38] School of Chemical Engineering, Sungkyunkwan University (SKKU), Suwon 16419, Korea.

[39] SPECIFIC, College of Engineering, Swansea University, Bay Campus, Fabian Way, SA1 8EN, Swansea, UK.

[40] Institute of Materials Science, Technical University of Darmstadt, Alarich-Weiss-Strasse 2, D-64287 Darmstadt, Germany

[41] Laboratory of Organic and Macromolecular Chemistry (IOMC), Friedrich Schiller University Jena, Humboldtstraße 10, D-07743 Jena, Germany.

[42] Clarendon Laboratory, University of Oxford, Oxford OX1 3PU, UK.

[43] Cavendish Laboratory, University of Cambridge, JJ Thomson Avenue, Cambridge CB3 0HE, UK.

[44] Skolkovo Institute of Science and Technology, Nobel St. 3, Moscow 143026, Russia.

[45] Institute for Problems of Chemical Physics of the Russian Academy of Sciences, Semenov Prospect 1, Chernogolovka 141432, Russia.

[46] Department of Materials, Imperial College London, London SW7 2AZ, UK.

[47] Department of Materials Science and Engineering, Yonsei University, Seoul 03722, Korea.

[48] Catalan Institute of Nanoscience and Nanotechnology (ICN2), CSIC and The Barcelona Institute of Science and Technology, Campus UAB, Bellaterra E-08193, Barcelona, Spain.

Key words: metal halide perovskites, perovskite solar cells, stability, ISOS protocols, standards, machine learning.

Abstract

We report a consensus between researchers in the field of perovskite solar cells (PSC) on procedures for conducting and reporting PSC stability testing. The International Summit on Organic Photovoltaic Stability (ISOS) protocols are re-assessed and extended for PSCs. In particular, the updated protocols highlight testing for: (1) Redistribution of charged species under electric fields, (2) distinguishing between degradation induced by various stress factors, and (3) reversible degradation. The recommended protocols are not for replacing existing qualification standards (e.g., IEC 61215), but rather to contribute to developing an understanding of PSC degradation mechanisms on research devices. Acceptance of these protocols and sharing the suggested datasets will facilitate inter-laboratory coordination will aid accumulation of PSC stability data acquired under well-defined and comparable conditions. This will allow the application of advanced approaches to analyzing large data sets, such as machine learning methods, and will accelerate the development of stable PSC devices.

1. Introduction

To ensure economic feasibility and competitive levelized cost of electricity, a new photovoltaic (PV) technology must achieve long-term stability. Desired durability can range from a few months to 25 years depending on the application, and is linked to the lifetime of the product in which the PV device is integrated (for example, the application range spans from disposable electronics to long-term facade elements). For power plants, the expectation for a PV module is 20 to 25 years of operation to match the reliability of currently employed silicon wafer-based modules. Halide PSCs are one of the most promising emerging PV technologies, especially when employed in high-efficiency multijunction architectures. The power conversion efficiency (PCE) of these potentially inexpensive, solution-processable devices has exhibited tremendous growth over the last decade, reaching 24.2% in a single junction PSC and 28% in a perovskite-on-silicon tandem [1,2]. The next major challenge for PSC technology, along with large area processing and manufacturing upscaling, consists in improving their reliability.

The degradation of PSCs is affected by multiple parameters, including the exposure to visible [3] and ultra-violet (UV) [4] light, high temperature, [5–7] contamination from the ambient environment (oxygen, humidity) [8–10] and electrical bias [11–13]. A detailed understanding of the various failure modes occurring during in-field operation of the solar cells is key to minimizing or even eliminating performance losses. Together with field tests, accelerated life-time (ALT) tests are of fundamental

importance to reduce the time to market of a new PV technology. Ideally, this requires sufficient understanding and verification that ALT testing indeed reproduces and amplifies only the failure modes observed under real operational conditions. Moreover, the acceleration factor should in principle be derived from a physical model such as, for example, the activation energy (i.e. the Arrhenius factor) in thermal ALT tests.

In 2011, a broad consortium of researchers developed recommendations for stability evaluation of organic photovoltaics (OPV) [14]. These standardized aging experiments are recognized as the "ISOS protocols", and were established at the "International Summit on Organic PV Stability (ISOS)" (Roskilde, Denmark; 2010). The ISOS protocols outline a consensus between researchers in the OPV field on performing and reporting degradation studies in a controlled and reproducible way, with fewer, yet more comparable testing conditions than those previously considered by the OPV community. The well-classified ISOS testing protocols and reporting requirements have subsequently allowed direct comparison of results between different research laboratories working on different solar cell designs, thus enabling successful round robin experiments, [15–17] and a comprehensive understanding of degradation in those devices.

Similar to the situation for OPVs several years ago, stability studies for PSCs are drawing increasing attention, as reflected by the growing number of publications on the topic and the increasing shift in emphasis of research in the field toward stability-related issues. Despite a large number of publications (over 3000 papers related to PSC stability only in the last three years), it is difficult to compare available results, mostly due to differences in the control and reporting of parameters as well as the inconsistent application of statistics to PSC stability data [18]. The time is now ripe for the development of unified PSC stability evaluation procedures [11,18–26], that the research community can broadly adopt, similar to the procedures recently developed for PSC efficiency measurements [27–30]. The ISOS protocols are an excellent starting point for unification of PSC degradation and stability testing, provided the particularities of perovskite solar cells are also addressed in the new protocols. The aim is to develop a consensus on standardized testing that enables consolidation of a large volume of published data into a single database. This can, in turn, be used to reliably compare stability studies, to analyze the relative significance of various degradation factors, and to ultimately identify key failure mechanisms in the devices. If the research community adopts a unified set of protocols in their experimentation and, perhaps more critically, in their reporting, a broad PSC stability database for different perovskite compositions (bandgaps) as well as solar cell layer stacks and architectures can be

accumulated over time, eventually allowing easier identification of common features. In turn, this can lead to the effective implementation of machine learning (ML) toward predicting lifetimes and failures [31].

The present work presents and extends the outcomes of a Round Table discussion of this issue that took place during the 11th International Summit on Organic and Hybrid Photovoltaics Stability (ISOS 11) in Suzhou, China in October, 2018 [32]. The manuscript is organized as follows: First, the published ISOS stress protocols are reviewed, highlighting their relevance for understanding PSC degradation pathways. Then additional stress tests that account for stability issues particular to PSCs, which are not considered by existing protocols, are proposed. Next, stability characterization methods and reporting standards are discussed. Finally, we consider the opportunities for data analysis arising from unified testing procedures on various devices by multiple research groups.

ISOS stability protocols are most frequently applied at the cell level, but their application to neat materials, "half" cells (incomplete PV stacks) and mini-modules can also provide valuable information on degradation processes. These protocols are not intended to be a standard qualification test, nor are they suited for application by industry or insurance agencies. Unlike qualification standards, the solar cell cannot pass or fail ISOS stability tests. Instead, these are research guidelines aimed at ensuring the comparability of solar cell testing performed at different laboratories, and therefore assist in improving the quality and relevance of published data in the field. The existing qualification tests described in the IEC 61215 and 61730 standards [33,34] were designed to apply to the field performance of silicon wafer-based solar panels to screen for well-understood degradation modes generally associated with conventional solar module level issues. These tests are unlikely to be well suited to *emerging PV* technologies (i.e., organic, dye-sensitized, halide perovskite, among others), due to their fundamentally different material properties and device architectures. In fact, today, various reports show that the stability of perovskite-based devices cannot be fully assessed by the procedures developed for conventional PV products. In particular, when testing PSC stability, special attention should be paid to 1) recovery processes after stress removal; 2) the presence of mobile charged species (ions); and 3) distinguishing the processes related to exposure to ambient atmosphere, from device-related, intrinsic factors. PSCs are also known to exhibit hysteresis in their current density-voltage (J-V) characteristics (i.e., a dependence of the J-V measurements on direction and rate of the voltage sweep [35,36]), which imposes constraints on the cell performance and stability characterization methods, but not necessarily signifies less stable devices[37]. The update to the ISOS aging protocols presented here reflects all mentioned features. In addition, we suggest reporting guidelines to facilitate data

aggregation and comparisons. To this end, we also advocate the reporting of performance of sub-optimized cells in addition to that of "champion" devices, as these data sets are critically important for training machine learning models.

2. Existing ISOS stability protocols

As noted by Christians et al., stability research should be performed at three connected hierarchical levels: material, solar cell, and solar module [21]. Many of the stress tests specific to encapsulated modules (such as hail test, PID, bypass diode stability etc. [33,34]), as well as mechanical stability and special consideration for space applications, are outside the scope of this report, and indeed will likely be leveraged from the existing IEC 61215 standard.

ISOS protocols designed for OPV are grouped by the applied stresses (see Table 1) [14]. Each group of the original ISOS protocols has three levels of sophistication, which aim at covering different levels of laboratory infrastructure. The first level requires only basic equipment providing lower control over the stress factors. The second and third levels require more specialized tools, such as environmental chambers and maximum power point (MPP) trackers, but provide a higher level of confidence in the results reported and, in most cases, more stringent test conditions. Explicit values in Table 1 stand for the controlled (i.e. monitored and adjusted) parameters. Note, that suggested protocols allow working with both encapsulated and unencapsulated devices as long as it is clearly reported (see detailed discussion in section 3.3).

Dark storage studies (**ISOS-D**) provide information on the tolerance of the solar cells to oxygen, moisture, other aggressive atmosphere components (e.g. CO_2, NO_x, H_2S, etc.) and elevated temperatures. In other words, ISOS-D tests give an estimation of the cell shelf life under ambient conditions without light exposure. Ambient atmosphere is crucial for the lifetime of perovskite absorbers and some of the transport layers used in PSC architectures [9,38,39]. Particularly, interaction with ambient species can promote the formation of traps [40] or charge barriers [41] (as a result of increased density of mobile defects/ionic species and electronic traps within the active layer) as well as perovskite decomposition, which quickly deteriorate device performance [8]. Atmospheric species were also shown to charge perovskite surface, affecting ions distribution across the device [42]. Elevated temperatures are used to study the thermal stability of the cell and to accelerate the degradation induced by other stressors [43]. Thermal degradation in the dark was observed in PSCs at elevated temperatures due to chemical and structural instabilities of the absorber materials [25,44] or transport layers [45,46].

Notably, some metal halide perovskites undergo phase transitions in the temperature range relevant for PV applications.[47,48] At the moment, the impact of phase transitions on the device lifetime is unclear, and so is the impact of different temperature regimes during (accelerated) aging. ISOS-D-1 tests *on-shelf stability*, where the cell environment is only monitored but not explicitly controlled (it is assumed that room temperature (RT) in the laboratory is 23±4 °C). Monitoring and reporting ambient relative humidity level is critical in all the protocols, since dry (R.H. < 20%) and humid air represent dramatically different stress conditions for PSCs[39,49]. ISOS-D-2 is a *thermal stability* test performed at controlled (i.e. monitored and adjusted) elevated temperatures of 65 or 85 °C. ISOS-D-3 is a *damp heat test* requiring accurate control of both temperature and humidity with the same temperature setpoints of 65 or 85°C and the introduction of 85% relative humidity.

In *outdoor stability* studies (**ISOS-O**), aging is achieved under illumination by natural sunlight at ambient environment. Although these conditions are not necessarily reproducible (they depend on weather, location, season etc.), the results of outdoor testing are the most relevant to the device operation. Unlike other protocols, they can be directly applied for realistic device lifetime assessment, albeit specific to a given climate. Field tests also allow determining whether the list of failure modes identified in the lab is complete and adequate for understanding reliability of the solar cell under real operating conditions, and further, can provide a reference point for acceleration factor calculations. A similar approach was originally pursued to rapidly accelerate the stability of Si modules through the Flat-Plate Solar Array project (FSA) using five "Block Buys" that directly correlated outdoor tests with having passed various qualification tests that ultimately helped form the foundation of IEC 61215 [50]. In this manner, in the FSA project from 1975-1985 outdoor module reliability was improved in a manner that reduced module failure rates from ~50% pre-Block V to ~1% for Block V [51,52]. To date, PSC outdoor stability studies are scarce [53–56], but the community has gained some critical insights with ISOS-O experiments, such as the importance of light/dark cycling [54] and the unexpectedly high open circuit voltage at low illumination intensities [55]. Under the ISOS-O-1 protocol, periodic measurements of J-V curves are conducted under illumination from a solar simulator. In ISOS-O-2, the J-V measurements are periodically acquired under natural sunlight. In ISOS-O-3 both in-situ maximum power point tracking under natural sunlight and periodic performance measurements under a solar simulator are performed.

The results obtained by J-V measurements and MPP tracking do not necessarily coincide in PSCs (Fig. 1a) [22], although they generally demonstrate similar trends [11,57]. Therefore, it is crucial for

PSC characterization to rigorously describe the load and recovery time before J-V measurements. MPP tracking is encouraged, whenever possible, both as the most practical electrical bias condition for aging and as a reliable tool for PSC performance assessment (see more discussion in section 4.1). However, it is mandatory only at the third, most advanced level of ISOS protocols. It is also possible to use a fixed voltage bias near MPP (instead of active MPP tracking) at lower sophistication levels, as suggested by the original ISOS protocols[14].

Light-soaking stability ("Laboratory weathering" in the original ISOS protocols[14]) experiments (**ISOS-L**) in PSCs have been found to promote ion and defect migration [58–63] as well as phase segregation [64,65] in the perovskite photoactive layer causing efficiency degradation. Additionally, light can catalyze/accelerate harmful chemical reactions, which lead to perovskite decomposition [66] or defect formation [67]. Detrimental changes in organic charge extraction layers, material intermixing at the interfaces, and ions exchange with adjacent solar cell layers can also be caused by cell illumination [61,68,69]. Similar to OPV [70] and DSSC [71], special attention should be paid to the spectral composition of the light source when studying PSC stability, particularly in the UV range. UV light was shown to assist perovskite decomposition [72] and increase the non-radiative recombination rate in PSCs based on mesoporous TiO_2, [73] which thus may require UV blocking layers to become more stable. PSCs with novel transport layers were shown to be tolerant towards UV irradiation [74,75]. Light from UV-A and UV-B spectral ranges may have different effects on PSC stability [76].

Thermal cycling (**ISOS-T**) in the dark and *light-humidity-thermal cycling* ("Solar thermal humidity cycling" in the original ISOS protocols[14]) (**ISOS-LT**) are more sophisticated protocols that evaluate the damage to photovoltaic devices caused by diurnal and seasonal variations of the weather in terms of solar radiation, temperature, and humidity. These tests are relevant to PSCs as for any other outdoor dedicated PV technology since they i) simulate realistic conditions, ii) stimulate failure mechanisms related to delamination of layers/contacts[77] and iii) are included in the qualification standards [78]. Particularly for PSCs, Schwenzer et al. demonstrated that the degradation under varying temperature is more severe than that under constant extreme temperatures, which was attributed to the effect of ions accumulation at the contacts [6]. Cheacharoen et al. solved a delamination issue from thermal cycling by adding a flexible polymer buffer layer around the mechanically fragile perovskite, which resulted in strengthening of the weakest organic layer within the PSC stack measured by the fracture energy and PSCs retaining more than 90% of their performance after 200 cycles between -40 to 85 °C[77]. Tress et al. applied temperature-illumination cycling, which resembles weather conditions

in central Europe during several representative days, to PSCs held in a nitrogen atmosphere [79]. This gave insights into the real-world operation of PSCs and emphasized the complex interplay of temperature-dependent transient effects during the day with reversible and irreversible degradation processes. Depending on the available equipment, temperature cycling varies from simple turning on/off the hotplate installed in an ambient environment, to complex temperature and humidity cycles inside an environmental chamber. Examples of the cycles can be found elsewhere [14,78].

Table 1. Overview of reported [14] and suggested ISOS protocols. The latter are printed in bold.

	Dark storage (ISOS-D)			Light-soaking (ISOS-L)		
Test ID	D-1	D-2	D-3	L-1	L-2	L-3
Light source	None	None	None	Solar simulator	Solar simulator	Solar simulator
Temp.	Ambient (23±4 °C)	65/85 °C	65/85 °C	Ambient (23±4 °C)	65/85 °C	65/85 °C
Rel. humidity	Ambient	Ambient	85%	Ambient	Ambient	~ 50%
Environment /setup	Ambient air	Oven, ambient air	Env. chamber	Light only	Light & temp.	Light, temp. & R.H.
Charact. light source	Solar sim. or sunlight	Solar simulator	Solar simulator	Solar simulator	Solar simulator	Solar simulator
Load	OC	OC	OC	MPP or OC	MPP or OC	MPP
	Bias stability (ISOS-V)			Outdoor stability (ISOS-O)		
Test ID	**V-1**	**V-2**	**V-3**	O-1	O-2	O-3
Light source	**None**	**None**	**None**	Sunlight	Sunlight	Sunlight
Temp.	**Ambient (23±4 °C)**	**65/85 °C**	**65/85 °C**	Ambient	Ambient	Ambient
Rel. humidity	**Ambient**	**Ambient**	**85%**	Ambient	Ambient	Ambient
Environment /setup	**Ambient air**	**Oven, ambient air**	**Env. chamber**	Outdoor	Outdoor	Outdoor
Charact. light source	**Solar simulator**	**Solar simulator**	**Solar simulator**	Solar simulator	Sunlight	Sunlight and Solar simulator
Load/ voltage bias	**Positive: V_{MPP}; V_{OC}; E_g/q; J_{SC} Negative: -V_{OC}, J_{MPP}** [a)]	**Positive: V_{MPP}; V_{OC}; E_g/q; J_{SC} Negative: -V_{OC}, J_{MPP}** [a)]	**Positive: V_{MPP}; V_{OC}; E_g/q; J_{SC} Negative: -V_{OC}, J_{MPP}** [a)]	MPP or OC	MPP or OC	MPP
	Thermal cycling (ISOS-T)			Light cycling (ISOS-LC)		
Test ID	T-1	T-2	T-3	**LC-1**	**LC-2**	**LC-3**
Light source	None	None	None	**Solar Simulator/dark Cycle period: 2, 8 or 24 h Duty cycle (light:dark): 1:1 or 1:2**		
Temp.	r.t. to 65/85 °C	r.t. to 65/85 °C	-40 to +85 °C	**Ambient (23±4 °C)**	**65/85 °C**	**65/85 °C**
Rel. humidity	Ambient	Ambient	**<55%** [b)]	**Ambient**	**Ambient**	**<50%**
Environment /setup	Hot plate/ oven	Oven/env. chamber	Env. chamber	**Light only**	**Light & temp.**	**Light, temp. & R.H.**
Characterization light	Solar simulator	Solar simulator	Solar simulator	**Solar simulator**	**Solar simulator**	**Solar simulator**

source						
Load	OC	OC	OC	**MPP or OC**	**MPP or OC**	**MPP**
	Light-humidity-thermal cycling (ISOS-LT)					
Test ID	LT-1 Solar-thermal cycling		LT-2 Solar-thermal-humidity cycling		LT-3 Solar-thermal-humidity-freeze cycling	
Light source	Solar simulator		Solar simulator		Solar simulator	
Temp.	Linear or step ramping between room temp. and 65 °C		Linear ramping between 5 °C and 65 °C		Linear ramping between -25 °C and 65 °C	
Rel. humidity	Monitored, uncontrolled		Monitored, controlled at 50% beyond 40 °C		Monitored, controlled at 50% beyond 40 °C	
Environment /setup	Weathering chamber		Env. chamber with sun simulation		Env. chamber with sun simulation and freezing	
Characterization light source	Solar simulator		Solar simulator		Solar simulator	
Load	MPP or OC		MPP or OC		MPP or OC	

OC stands for open circuit condition; MPP – maximum power point.

[a)] V_{OC}, V_{MPP}, and J_{MPP} are determined from light J-V curves measured under standard solar cell testing conditions on a fresh device. E_g and q are the bandgap of the active layer and elementary charge, respectively.

[b)] Relative humidity is controlled at temperatures above 40 °C, and uncontrolled for the rest of the cycle.

3. Suggested new ISOS protocols relevant for PSCs

Recently some aging protocols for PSC were suggested [25,27]. Mostly, they feature subsets of the original ISOS protocols described above, although some additional ideas, particularly concerning electrical bias application [25], have also been introduced. Below we suggest extensions of the aging procedures that particularly pertain to the unusual properties of halide perovskite PV. While a major part of the original purpose behind the ISOS protocols was to limit conditions for each level to facilitate more ready comparison, there is limited data on the following protocols. We propose a reporting framework, some example conditions, and a discussion as to why these might be relevant. A similar framework is likely to be useful for OPV and other emerging PV technologies. If these protocols become widespread over the next few years, the community can adopt a more informed decision on a limited number of consensus conditions.

3.1 Light/dark cycling (ISOS-LC)

Some PSC degradation modes have repeatedly been shown to be reversible (entirely or partly) in the dark (often referred to as metastability) [6,37,54,60,67,80–83]. Therefore, cycling of light/dark periods to simulate the day/night cycle produces a significantly different stress test than under constant illumination (ISOS-L) [11,54]. Two opposite types of dynamics have been demonstrated in the literature: photo-induced degradation with recovery in the dark [60,67] (Fig. 1c) and reversible photo-induced PCE increase with its subsequent decrease in the dark [54,82] (Fig. 1b). In particular, reversible performance losses are attributed to cations redistribution [60], metastable defects formation [67] or reversible chemical reactions [66]. The effects of PCE improvement under illumination after storage in the dark are commonly attributed to the neutralization of interfacial defects by photogenerated charge carriers or changes in the built-in electric field due to ion migration [84]. The PCE dynamics during the cycle were shown to change with status of the cell degradation [81]; for example, the term "fatigue" was introduced for slowing down of PCE restoration with each consecutive cycle (Fig. 1b) [82]. Such metastability is attributed to the migration of ions, which is known to be pronounced in metal halide perovskites [83]. Reversible and irreversible degradation mechanisms may co-exist in a given PSC [79,81,85].

ISOS protocols revised for perovskite PV should, therefore, include a group of light/dark cycling protocols to account for the recovery phenomena (**ISOS-LC** in Table 1). For the ISOS-

LC experiments, we suggest exposing the cell to simulated sunlight turned on and off with cycle periods 2, 8 or 24 h and duty cycles (light:dark) of 1:1 or 1:2. Among suggested conditions, 24 hours-long cycles (12 h light /12 h dark or 8 h light / 16 h dark) mimic the diurnal sun cycle. However, as the interplay between degradation and recovery in realistic conditions can be complex [79] and dependent on the cell history, varying cycle duration and the duty cycle is expected to provide additional information onto the extent of reversibility and sufficient recovery times. At the ISOS-LC-1 level, the cell should be kept at ambient conditions while the temperature and relative humidity are monitored, but not controlled. At the ISOS-LC-2 level, the cell is kept at fixed setpoint temperature of 65/85 °C in ambient atmosphere. At the ISOS-LC-3 level, relative humidity is controlled at 50% in addition to elevated temperatures. The sample atmosphere and required equipment are similar to corresponding ISOS-L protocols [14].

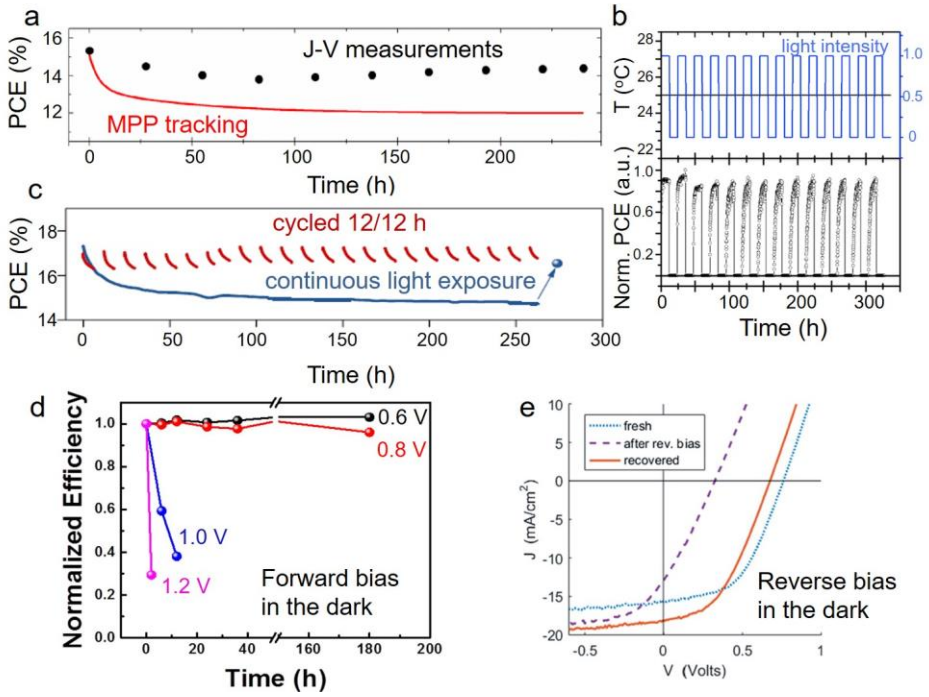

Fig. 1. Specific features of PSC stability studies. (a) PCE extracted from continuous MPP tracking (red line) versus periodic J-V scans collected from forward to reverse bias (black circles) for the same PSC. Adapted from [22] with permission of Elsevier. (b) Normalized PCE of PSC subjected to repeated 12 h light

on/off cycles at 25 °C and 10% relative humidity. Adapted from [82] with permission of Elsevier. (c) PCE evolution of PSCs exposed to continuous (blue line) or cycled (6/6 h, red lines) illumination by white LED. Adapted from [11] with permission of Springer Nature. (d) Normalized PCE changes of PSCs exposed to different forward bias in the dark. Adapted from [13] with permission of American Chemical Society. (e) Light J–V curves of a PSC when it was fresh, after 1 min at −20 mA/cm^2 and after recovering for over 3 h of maximum power point tracking. Adapted from [86] with permission of John Wiley and Sons.

3.2 Electrical bias in the dark (ISOS-V)

Electrical bias is shown to cause PSC degradation (which is also affected by the presence of other stress factors) [12,13,86,87]. The degradation, in this case, is commonly initiated by ion migration [13] or charge carriers accumulation resulting in detrimental electrochemical reactions [9]. Electric field is also shown to assist moisture-initiated perovskite degradation [87,88] since moisture ingress can result in the formation of hydrated perovskite phase containing mobile ions, whose drift accelerates the degradation [89]. Both positive (Fig. 1d) and negative (Fig. 1e) biases were shown to be potentially harmful [13,86] and might be realized during the solar panel operation. In our view, ISOS protocols revisited for perovskite photovoltaics should include ISOS-V group of testing in which the behavior of the cell is analyzed under exposure to certain electric bias in the dark (see Table 1).

Usually, the solar cell is kept near its MPP (i.e., positively biased with voltage < V_{OC}), however, disconnected cells under illumination would be biased at open circuit voltages (typically, ~ 1 V for iodine single junction PSCs). We, therefore, suggest applying voltage equal to V_{MPP} or V_{OC} (as measured under AM1.5G illumination condition on fresh device) as a positive bias condition. Since bias-induced effects may have a threshold behavior[13], we recommend voltages below E_g/q to avoid unnatural overstressing. Furthermore, a new protocol for assessing light-induced degradation (LID) in silicon modules will be introduced to IEC 61215. This will be applied to modules, which fail to stabilize in the efficiency measurement. However, instead of exposing the modules to light, they will be held under forward bias, such that the dark current density matches J_{SC}. This condition was shown to mimic MPP under full sun exposure for silicon modules. While there is no similar data for PSCs, such stability test might be also useful.

In case of the partly shaded solar module (by clouds, dirt, nearby trees etc.), shaded cell(s) can be forced to operate under reverse bias to match the current flow through the rest of the module [86,90,91]. The choice of negative bias stressing conditions depends on the anticipated module connection scheme, particularly on the use and choice of bypass diodes. At the moment there is no relevant understanding and experience for perovskite PV, therefore it is reasonable to learn from both types of experiments: with a constant negative bias applied (e.g., $-V_{OC}$), relevant for modules with bypass diodes, and with forcing a current up to $-J_{MPP}$ (which in the dark would mean relatively high negative bias applied to the cell). The latter condition simulates the situation of a partially shaded module in the absence of a bypass diode. Practical negative bias condition will depend on the details of the anticipated module layout.

Three sophistication levels differ by the level of control over the sample temperature and atmosphere and required equipment, which is similar to that in corresponding ISOS-D protocols (Table 1) [14].

Electrical bias application can cause a redistribution of charged species across the PSC, which might be reversible after the stress removal [13]. Thus, it is recommended to trace the cell recovery after the end of aging by storing it in the dark under open circuit (disconnected) condition and periodically checking its performance until it reaches saturation. For a similar reason, it might be challenging to ensure the steady state of J-V curve measurement after electrical bias stressing. We, therefore, recommend using MPP tracking (or stabilized current at a constant voltage close to MPP for ISOS-V-1 and ISOS-V-2) to account for possible transient effects. It might be also informative to report in-situ dark current (or voltage in constant current density mode) evolution during the stressing in addition to periodic J-V measurements in ISOS-V protocols.

3.3. Intrinsic stability testing (ISOS-I)

The stress factors can be divided into two groups: (1) *Intrinsic factors* including light, temperature and electrical bias (relevant regardless of the cell encapsulation/protective environment), and (2) *extrinsic factors* governed by the cell interactions with such ambient species as oxygen and/or moisture (which are relevant assuming imperfect device encapsulation).

Generally, “encapsulated” devices refers to the protection of the solar cells by gas-barrier materials, delaying the contact between the solar cell and ambient air (especially moisture which may be the most harmful species degrading the solar cells). Encapsulation can be performed by glass/glass sealing, lamination of rigid or flexible gas-barrier materials, direct deposition of protective layers (for example, dense layers deposited by atomic layer deposition or plasma enhanced chemical vapor deposition) or by a combination of the above-mentioned processes. Extrinsic stability is dependent on the barrier properties of encapsulation materials (along with device sensitivity towards air and chemical compatibility between encapsulation materials and device). In order to fully understand encapsulated device degradation, knowledge of gas barrier properties and their stability appear crucial. Specific characterization tools exist to measure gas barrier properties of encapsulation materials and to quantify the amount of moisture that has permeated orthogonally [92–95] and laterally[96,97] within the encapsulation. Such tools allow characterizing (and possibly improving) the encapsulation, independent of other device studies. The measurement of the lateral permeation from the edge of the encapsulation should mimic, to the extent possible, the operational encapsulation and take into account the interfacial permeation that is not considered in gas barrier measurement of bulk materials (this issue is particularly important if sealing materials are employed). The control of the self-resistance of encapsulation materials is particularly important as aging tests (high temperature, high humidity, UV) could cause degradation of the gas barrier protection and dramatic drops of the PV performance. Therefore, it is recommended to age encapsulating materials with the same aging conditions as encapsulated devices and to determine the gas barrier properties after aging. Development of dedicated encapsulation procedures constitutes a separate technological challenge, especially for PSCs [77,98–101].

In the vast majority of studies, barrier properties of the encapsulant are unknown, which inhibits the ability to differentiate between intrinsic and extrinsic solar cell stability. Even if the device is nominally “unencapsulated”, the top evaporated electrode can play the role of a barrier (once again, with unknown properties). This has motivated many research groups to focus on intrinsic PSC stability by stressing the cells *in an inert atmosphere*, for example within sealed pouches, or with equipment installed in the inert atmosphere glove-boxes or environmental chambers. This approach has brought about important insights onto PSC degradation

mechanisms, and is helpful in separating the impacts of thermal stresses, light, bias, and their cycling on the device degradation [11,102,103].

Table 2. Overview of suggested ISOS-I protocols for aging experiments in an inert atmosphere.

Test ID	Short description
ISOS-D-1I	Inert atm.; RT; dark
ISOS-D-2I	Inert atm.; elevated T; dark
ISOS-L-1I	Inert atm.; RT; light
ISOS-L-2I	Inert atm.; elevated T; light
ISOS-V-1I	Inert atm.; RT; dark; electrical bias
ISOS-V-2I	Inert atm.; elevated T; dark; electrical bias
ISOS-LC-1I	Inert atm.; RT; cycled light
ISOS-LC-2-3I	Inert atm.; elevated T; cycled light
ISOS-T-1-3I	Inert atm.; cycled T; dark

Accordingly, the new family of ISOS standards should be included for the studies of intrinsic stability under a specific stressor conducted in an inert atmosphere (nitrogen, argon etc.). Index "I" is used at the end of the protocol name (see Table 2) to indicate the change of atmosphere in the corresponding test to the inert one, while other parameters are kept the same. For example, ISOS-L-1I stands for intrinsic photo-stability at room temperature (similar to ISOS-L-1 except for the atmosphere), ISOS-L-2I – intrinsic photo-stability at elevated temperature, etc. The latter protocol is very important as it is often chosen to demonstrate the lifetime of a given PSC in research papers. Notably, the new protocols family includes aging experiments with a single stress factor (only heat in ISOS-D-2I; only electrical bias in ISOS-V-1I; only light in ISOS-L-1I etc.), which simplifies the analysis of degradation modes.

We note that encapsulation not only inhibits reactions with ambient species, but may also prevent out diffusion of volatile perovskite decomposition products from the module. Similarly, it was recently demonstrated that ultra-high vacuum conditions accelerate the light-induced degradation of unencapsulated perovskite cells [104]. There are further related complications due to the observation that oxygen plays a positive role in passivating deep traps levels in lead halide perovskites, but only at a very low partial pressure.[105] Therefore, encapsulated PSCs may have a superior lifetime, compared to the unencapsulated samples, even for degradation experiments conducted in an inert atmosphere. Additionally, the environment in which the encapsulation is

performed may also play a role. Thus, reporting the presence/absence and details of the encapsulation is mandatory also in "I" protocols.

4. Reporting stability studies

4.1. Checklist for PSC stability studies

For comparison and reproducibility of results, it is crucial to report sufficient information about the aging experiments, in addition to a detailed description of the device preparation [18]. Table 3 is a suggested checklist for stability data reporting, in accordance with that required by *'Nature'* journals for reporting PSC PV performance data [106]. We stress that even if a parameter is not controlled during the aging experiment (for example, temperature or relative humidity (stating if this is the value in the laboratory at room temperature, or in the aging apparatus) on the first level of ISOS protocols), it is still important to monitor and report the parameters listed in Table 3.

We recommend that researchers should specify the number of samples studied in each aging condition. According to critical analysis on the quality of PSC stability studies reported by Tiihonen and co-workers [18], nearly half of the studies consider only 1 sample of each kind, which is particularly worrisome for PSCs typically characterized by relatively low reproducibility. Ideally, statistics should be provided to account for sample-to-sample and batch-to-batch variations. The same work provides estimations of the desired sample size [18].

Stability data are often reported as normalized parameter evolution with aging time, while only specifying the performance of a representative fresh device (champion or average). Thus, the reported stabilities and efficiencies may be measured on different devices and, therefore, cannot be directly related. Any plot with normalized parameter variation should include the value to which it is normalized [23].

Due to the ongoing development of best practices for J-V and efficiency measurements on PSCs [27–30,107], the procedure for periodic measurements during the aging test should be clearly described. Typically, measurements of the J-V curve (or part thereof) are taken with certain

periodicity depending on the characteristic degradation timescale of particular devices. Since J-V hysteresis is common in PSCs, steps should be taken to ensure the measurements are taken under (quasi) steady-state conditions. This can usually be achieved using a dynamic J-V approach [28,108], which allows time at each voltage step for the current to settle (stabilize), or alternatively, using a very slow J-V scan in the vicinity of the maximum power point, usually repeated in the reverse direction to check for consistency. If suitable equipment is available, a third approach to logging the steady-state performance of the device over time is maximum power point tracking (MPPT) [20,29,36]. MPPT can be particularly effective, since it simultaneously holds the device at its normal operating voltage and measures the output. Due to hysteresis however, standard perturb-and-observe (P&O) MPPT algorithms might be suboptimal for PSCs [109]. Modifications of a P&O algorithm were suggested for effective MPPT in solar cells exhibiting hysteresis, including extended (asymmetric) thresholds for switching the voltage sweep direction[109] and predictive MPPT algorithms with lowered settling times [110,111]. If any form of MPPT is used during an experiment, the hardware and MPPT algorithm should be clearly referenced. Similar to OPVs[112], preconditioning the PSC (with light and/or electrical bias) prior to each J-V scan may affect the outcome and should be reported. Additional non-destructive characterizations at the intermediate stages of PSC aging are encouraged, though care must be taken to account for possible cell recovery during the time of the measurements.

MPPT is also recommended as a bias condition for aging experiments conducted under illumination while being mandatory only at the third sophistication level. When MPPT is performed throughout the entire aging test, it is recommended to periodically measure J-V curves, since these measurements provide more detailed information on the degradation mechanism. Additional non-destructive characterizations at the intermediate stages of PSC aging are encouraged, though care must be taken to account for possible cell recovery during the time of the measurements.

For every light source an irradiance in the range 800-1000 W/m² should ideally be applied, and the exact value of irradiance reported. Another important factor to be considered during aging experiments is the type and spectrum of the light source used. Table S1 shows a collection of the most stable reported PSCs to date that withstand more than 1000 h of light-soaking while losing less than 15% of their initial PCE. As follows from Table S1, five main

types of light sources were used: a) Sulfur plasma lamp, b) white Light Emitting Diodes (LED), c) metal halide/Xenon Lamp, d) "solar simulator" and e) "outdoor" (i.e., real sunlight). The "solar simulator" section (Table S1, section d) encompasses many devices analyzed under unspecified conditions of irradiation. Sulfur plasma and white LED illumination typically do not include UV light and thus it is redundant to report the use (or not) of a UV filter (except for the modern LED sources with extended range, which may have components in 300 to 400 nm range); reporting that "no UV filter was applied" is misleading in this case. Metal halide and Xenon arc lamps include UV light and thus, their use requires reporting the application of a UV (or any other) filter. Reporting the company and model of the solar simulator is good practice (one can refer to the company's online information). Note that ASTM's class "A" for simulated solar spectrum is relevant between 400-1100 nm only[113]. Therefore, the type of light source used and its spectrum (as supplementary materials) should always be clearly specified. Reporting "AM 1.5G illumination" without specifying the light source, the solar simulator details and the calibration procedure, is not sufficient.

Furthermore, that some of the light sources described above (especially Xenon lamps) may degrade significantly on the timescale of the stability experiments. It is recommended to periodically check the light intensity with a reference cell and correct if needed.

There are reports that PSCs, as well as DSSCs [114,115] and OPVs [116–119], might be suitable for indoor and outdoor low light intensity applications [120,121]. Indoor light illuminance is significantly smaller (100 to 200 lux in a typical home, and 250 to 1000 lux in an office [122], which corresponds to roughly 1% of 1 sun irradiance). Spectra of indoor light sources are also significantly different from natural sunlight and there is still no standard spectrum for indoor solar cells testing [123]. Artificial indoor light sources can be roughly divided into four different categories: a) Black Body (incandescent bulbs, "warm" white light); b) Compact Fluorescent Lamp, c) white LEDs and d) High Pressure (e.g. phosphor, sodium, mercury) lamps [124]. Among them, LEDs are predicted to increase the share of indoor lighting market due to their high lighting efficiency [125]. For PSCs intended for low-intensity illumination, we encourage device characterization at several intensity levels (e.g. 200, 500, 1000 lx) and reporting the light source (preferably, LED) spectrum in accordance with original ISOS procedures [14].

Table 3. Suggested checklist for reporting experimental stability test data.

Initial cell characterization: Current-voltage (J-V) curves of fresh devices, including voltage scan conditions (scan speed, direction, dwelling time, the number of power line cycles (NPLC), preconditioning etc.); stabilized photocurrent at MPP or MPP tracking data of fresh device; EQE/IPCE spectra (indicating the lock-in frequency and light bias if used, and if monochromatic light is smaller than active area, or larger and optical mask applied) and its comparison to J_{SC} obtained from J-V data.
Encapsulation: Wiring (materials, processing conditions, addition of a protective sealant); front and back side encapsulation layer(s) (materials (reference or composition, thickness), processing conditions (environment, temperature, duration)); edge sealant (materials (reference, thickness, width), processing conditions); geometry (rim (minimum distance between encapsulation edge and active area edge); device active area; picture or a scheme of the device).
Aging conditions: The light source used in the aging experiment (light source type, intensity, spectrum, filters applied, calibration); light cycling (if applicable). Temperature (in shadow and/or under the illumination, measured with thermocouple or black standard temperature sensor). Atmosphere (air/ glovebox/ sealed pouch/ environmental chamber etc.; controlled or monitored). Electrical bias condition (open circuit/ maximum power point/ short circuit/ constant load). Conditions cycling (dwell and period times), if applicable. Do your test conditions comply with known protocols (IEC/ ISOS etc.)?
Aging time: Exposure time to stress conditions; performance loss observed during that time, resting times (e.g. without stress).
Measurements during aging: Periodically recorded J-V curves (recording frequency, scan speed, direction, NPLC, dwelling time, preconditioning, etc.), recovery time and conditions, maximum power point tracking (including tracking algorithm), and other periodic measurements if applied.
Number of samples: Number of solar cells of each type tested in each aging condition, statistical analysis (if applicable). Number of samples still operating above a specified efficiency level at the end of the aging test.
Outdoor stability: Location (city/coordinates) and dates of exposure, the weather conditions (temperature, humidity, sunlight irradiance) throughout the exposure period, preferably in tabulated format.

4.2. Stability figures of merit and acceleration factors

The time corresponding to efficiency drop to below 80% of its initial magnitude is commonly referred to as T_{80}. T_{80} often serves as a figure of merit (FOM) of solar cell stability; it, therefore, would be optimal as the minimum aging test time. Despite the apparent simplicity, there are several approaches[126,127] to determine device T_{80} (see Fig. 2 and Table S2 for a summary). It is, therefore, of vital importance to describe in details metrics used when reporting stability studies. In particular, the original ISOS protocols[14] suggested the use of stabilized T_{S80} time, the time during which the PCE decreases by 20% of its magnitude after an arbitrarily defined stabilization time (blue color lines in Fig. 2). This suggestion is based on the widely known shape of 'PCE versus time' curve in OPVs with rapid initial degradation ("burn-in") [127] followed by a stabilized region. While similar dynamics have been observed in some PSCs [11,128,129], it is not a universal trend for these devices (Fig. 3) and, thus, should be applied in cases where it is relevant. In case of non-monotonous PCE changes (see examples in Fig. 3), we recommend calculating T_{S80} starting from the time of observation of maximum efficiency. Third available strategy for T_{80} determination is similar to T_{S80} (green lines in Fig. 2), but includes the "burn-in"/light soaking time into the lifetime FOM and suggest a linear back extrapolation to redefine starting PCE in case of curves with "burn-in" effect [130]. If properly applied, extrapolation of aging data (or readily achieved T_{80} lifetimes) can be used to evaluate another highly relevant parameter for particular application scenarios: by combining the power conversion efficiency with lifetime, the lifetime energy yield (LEY) can be calculated [127]. This helps in comparing energy invested into device production with expected energy output, a parameter relevant for life cycle analysis.

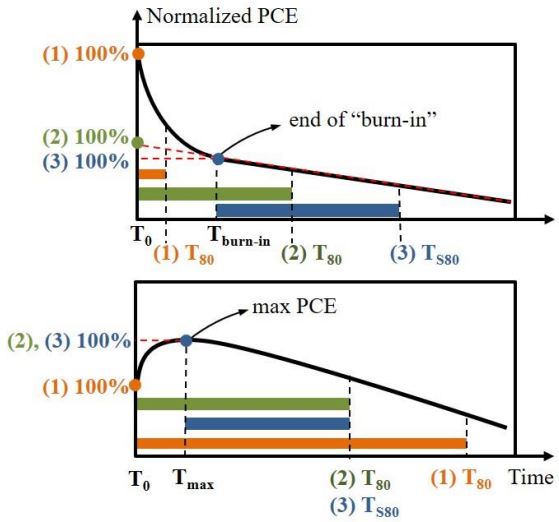

Fig. 2. Possible practices for T80 estimations (the time of PCE decrease by 20% of its initial value). The black curves schematically show PCE evolutions with aging time in the case of "burn-in" effect (a) and in the case of non-monotonous PCE changes (b). Three depicted strategies for T80 estimations differ in the way the initial PCE is estimated ("100 %") and the starting point of the aging timer (shown in the figure as circles of corresponding colors). (1) 80% is counted from the initial PCE at $t=T_0$; shown in orange color. (2) 80% is counted from back-extrapolated PCE value (a) or from the maximum value over the experiment (b); the timer starts at $t=T_0$; shown in green color. (3) 80% is counted from PCE value at $t=T_{burn\text{-}in}$ (a) or at $t=T_{max}$ (b), the time starts at corresponding timestamps; shown in blue color.

The T_{80} of the most stable PSCs have been demonstrated to exceed 1,000 hours (42 days) or even 10,000 hours (>1 year) for 2D-3D perovskites [131] under certain stress conditions including illumination [58,128,132]. Considered recent advancements in PSCs stability (see also table S1), we strongly recommend that reviewers and journal editors discourage the use of word "stable" in the title of scientific papers if they don´t match the state of art in terms of efficiency losses and harshness of aging conditions (1000 h under 1 sun illumination with PCE decrease less than 20% as a rule of thumb). Notably, such long exposure times are challenging to realize. If T_{80} is not reached, it is difficult to predict the lifetime based on the observed 'PCE versus time' trend, due to the variety of curve shapes observed (Fig. 3). In this case, we suggest

performing aging for at least 1000 hours and using the PCE after 1000 hours of stress (η_{1000}, as a percentage of the initial PCE) as stability FOM. If authors choose to apply any kind of

extrapolation to determine T_{80} or T_{S80}, it must be clearly distinguished from the measured data. In this case, it is recommended to limit the extrapolation times to below one order of magnitude larger than the actual aging time. As the stability of PSCs improves, it may become common to quote T_{95} values, the lifetime to degrade to 95% of the starting efficiency, for the more stable cells. This will also be in keeping with the IEC procedures, where the pass-criteria is for the modules to operate at >95% of their starting performance after the stress exposures.

The presence of reversible degradation in PSCs complicates their stability assessment. There are no broadly accepted FOMs accounting for partial reversibility at the moment, however, some procedures are currently debated [22,54]. Recovery effects can be studied in two types of experiments: 1) Continuous aging followed by the performance tracing after the stress removal, or 2) cycled stress experiments. In the former case, it was suggested to correct T_{80} accounting for the amount of restoration occurring during the rest period [22]. In cycled experiments (such as ISOS-LC), an analogue of T_{80} metric might be introduced for the energy output per cycle[54].

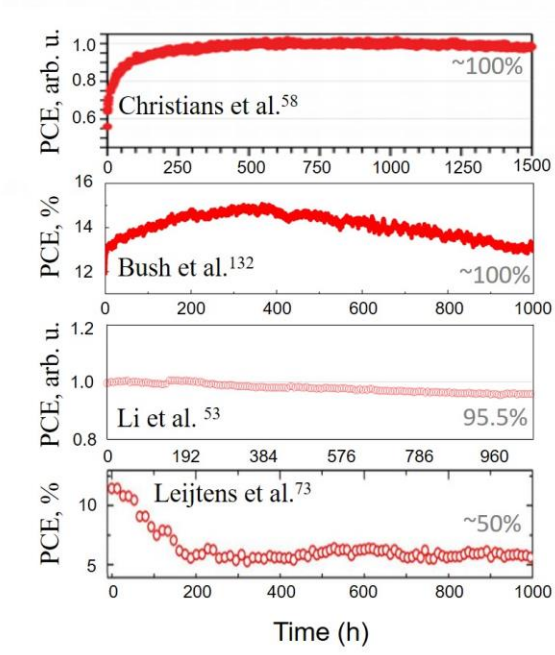

Fig. 3. Examples of the best PSC's stability reported so far, demonstrating a variety of possible PCE evolution trends upon aging under 1 sun illumination. Adapted from [53,58,73,132] with permission of Springer Nature and John Wiley and Sons.

The ISOS testing protocols do not provide direct information on the expected lifetime of the solar cell under operational conditions. For such evaluations, the concept of Acceleration Factor (AF) was previously utilized [133]. AF is a constant, which relates the times to failure under accelerated and reference (operational conditions) stress tests. Once the AF is determined for an aging protocol, the accelerated test can be used to estimate cell lifetime in a fast and reproducible manner in the laboratory. For this, the aging conditions used for testing should only accelerate the degradation modes active under real-world operation. To date, no reports have been made of AFs of PSCs subjected to accelerated aging. However, attempts to deduce AF for accelerated aging of OPVs have been more widespread [43,133,134] and reports for PSCs are anticipated to appear as the technology matures. Kettle et al. have deduced AFs for most ISOS tests relative to outdoor conditions in northern Europe using OPV mini-modules [133]. Overall, it was shown that dark storage ISOS-D tests could yield AFs between 0.45 (ISOS-D-1) and 12 (ISOS-D-3). Light soaking ISOS-L tests showed an AF of 15 and 24 in ISOS-L-1 and ISOS-L-2 tests, respectively.

To further speed up the development of stable PSCs, using a high-intensity light has been suggested [19,135–138] and utilized for degradation studies of perovskite absorbers [135] and solar cells [137] with intensities up to 100 and 10 suns, respectively. Rough estimates show that even moderate light intensities of several suns can tremendously accelerate the degradation. For example, Boyd et al. estimated that operating the solar cell for 1000 h under continuous illumination with an intensity of only 5 suns under 85 °C would provide an equivalent of tens of years of outdoor testing if degradation scales linearly with light intensity [19]. Such intensities are easily achievable with commercial light sources and solar concentration.

High light intensities (up to hundreds of suns and beyond) can provide substantially higher acceleration factors, which may be required to assess the durability of future generations of stable PSCs. However, such tests require careful independent control of cell temperature and illumination intensity [139,140]. Moreover, care should be taken to check whether the degradation mechanisms occurring under high light intensity and under 1 sun are identical. To the best of our knowledge, such studies have not been reported for PSCs. However, corresponding experiments

with OPVs under concentrated sunlight (both polymer- [141] and small molecules-based [134,142]) revealed that increasing the light concentration from 1 sun to 100 suns did not change the degradation mechanisms. Similar results were obtained using high intensity simulated sunlight [142,143] with OPV lifetimes of tens of years predicted in each case.

5. The significance of consensus for further research and data analyses

As ISOS protocols are intended for research purposes, a variety of testing procedures is suggested (see Table 1) concerning the four major degradation factors: atmosphere, temperature, electrical bias, and light. Table 4 shows a graphical representation of the corresponding aging test details, which can be used to study the effect of these factors and their combinations. For each combination of light and bias, 9 types of aging protocols might be suggested with respect to temperature (ambient; elevated or cycled) and atmosphere (ambient; controlled humidity level or inert). Apart from determining the lifetime of a given solar cell at specific conditions, additional information on the impact of the stress factors might be gained by comparing the results of different aging procedures to each other. For example, comparison of D-1 and D-2 protocols will provide insight on the effect of elevated temperature; D-2I, D-2 and D-3 – the effect of an atmosphere; D-2 and L-2 combined effect of light and heat etc. Arrows aside Table 4 schematically depict these relationships.

The many blank spaces in Table 4 can be filled with corresponding aging procedures (by analogy with additional ISOS tests suggested in section 3) in a straightforward manner. Other protocols can be constructed by varying "fixed" parameters (e.g. temperature, light intensity, R.H.). We do not aim to cover all the possibilities with ISOS protocols nor discredit studies with a systematic variation of a particular stressor. Nevertheless, these investigations would benefit from having common "reference points" with other studies conducted at different laboratories, device architectures, perovskite materials, and even different research questions in mind. Consensual conditions, like ISOS protocols, may serve as such references.

Having unified procedures of stability studies with an easily machine-readable reporting structure could also lead to the creation of a large database that allows for more statistically reliable comparisons. Such a database is necessary to identify patterns in the data, and deduce

rules and heuristics for future work. Although the analysis of such large data sets will not be easy with the use of traditional approaches, statistical machine learning methods can enable important trends to be discovered [31,144,145]. These methods will be facilitated if abundant and uniformly-reported data sets are available. As indicated in Fig. 1, having enough data becomes less of an issue with a growing number of papers published in recent years. Unfortunately, this is not yet true for shared protocols. For example, in a previous work involving machine learning analysis of PSCs efficiencies, only 26% of 1921 randomly collected data points also contained steady-state efficiencies measured with MPP tracking; even the protocols for these measurements were not completely uniform [144]. However, this data subset resulted in better machine learning (ML) models compared to the entire dataset. The situation seems to be worse in stability related publications: in addition to unique measurement protocols, the storage conditions of the samples (which are also vital to assess the degradation process) are also not uniform, and not properly reported in a significant number of papers. These considerations make the requirement for consensus protocols even stricter for stability studies.

Determining the role of each stressor on device performance through ML methods could enable a direct comparison between results from different research laboratories around the world. Briefly, by using information from aging measurements under the relevant stressors, as discussed above, one can optimize the steps needed for supervised learning algorithms. The PCE values obtained from aging tests are ideal training data and can be utilized for supervised learning. A so-called feature vector is implemented based on this data, and then the derived values are used as input for an artificial neural network or other machine learning tools. Ultimately, the reliability of ML strongly relies on having sufficient information (quantity and diversity) from aging tests that can provide an accurate prediction of device performance and degradation. Thus, the ML algorithms must be trained with extensive laboratory data, where prediction values can be compared to actual performance measurements. Once working, ML tools should provide knowledge extraction without the need to perform all tests presented in Table 4. Note that while the same ML algorithm can be implemented to predict the behavior of any type of perovskite, we anticipate that new datasets of aging measurements are needed for the distinct chemical compositions, considering the broad variability of performance dynamics for each. In order to accommodate the large number of perovskites possibly suitable for PV, a shared-knowledge repository database has been proposed [31], where positive and negative results (i.e., not only

champion cell, but also the suboptimal or underperforming devices aged under similar conditions) from stability tests are considered equally important for ML, as they all represent valuable training data. It is therefore critical that a trend emerges that all cells put into an aging test are measured and report for the duration, even total failures. At a research laboratory scale, this information could be shared if researchers identify the conditions utilized for perovskites' fabrication and testing through a common website. The progress in this direction might be significantly accelerated if the researchers, who foresee their data being useful for ML, would provide complete information (on device's fabrication, performance and stability) in standardized tabulated format (a possible template can be downloaded from SI). A similar strategy can be extended from PSCs to OPV and other emerging PV systems. Potentially, ML trained on a sufficiently extensive database can allow detecting statistically significant stress factors, correlating repeated phenomena in different studies towards detecting universal degradation phenomena and stabilizing approaches, and predictions of lifetimes and failure modes.

Table 4. Stress factors affecting the solar cell in different ISOS protocols.

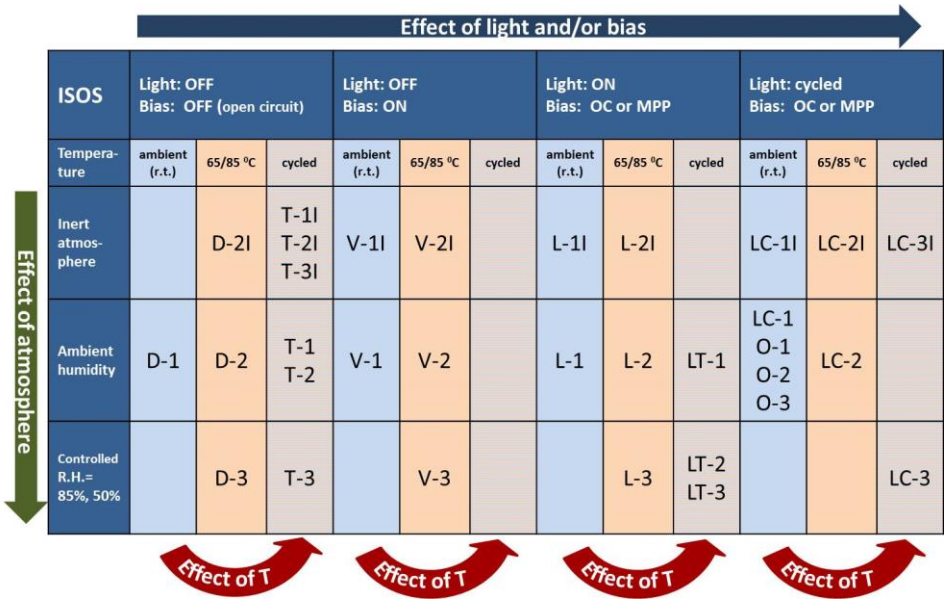

Summary and Conclusions

This paper reports a consensus on procedures for perovskite solar cell stability studies discussed at the 11th International Summit on Organic and Hybrid Photovoltaics Stability (ISOS-11). Suggested protocols primarily rely on the original ISOS standards developed for OPV [14], which have been shown to be highly relevant for uncovering various degradation pathways in PSCs. We further suggest extending the set of protocols in accordance with specific stability features of PSCs, including: 1) light/dark cycling (ISOS-LC) mimicking the diurnal cycle; 2) study of the cells behavior under continuously applied bias in the dark; 3) protocols for intrinsic solar cells stability studies (indexed with "I"). These tests have already proven their usefulness in understanding PSCs failure modes. We also propose a checklist for uniformly reporting results of PSC stability studies. This list ensures that the research can be reproduced and compared with results from other laboratories. Procedures and good practices for stability tests are discussed.

We expect that the guidelines for conducting and reporting stability studies described in this paper will improve comparability between data from different laboratories and device architectures. The set of procedures and practices suggested here serve as an intermediate stage in perovskite solar cells technology maturing, aimed at the identification of degradation pathways and the prospects for their mitigation. If broadly accepted, these quasi-standards would significantly speed up stability data accumulation, which can be utilized for predictive machine learning to further facilitate the development of stable and reliable PV devices.

Acknowledgements

This article is based upon work from COST Action StableNextSol MP1307 supported by COST (European Cooperation in Science and Technology). M. V. K., E. A. K., V. B. and A. Osherov thank the financial support of the United States – Israel Binational Science Foundation (grant no. 2015757). E. A. K., A. A. and I. V.-F. acknowledge a partial support from the SNaPSHoTs project in the framework of the German-Israeli bilateral R&D cooperation in the field of applied nanotechnology. M. S. L. thanks the financial support of NSF (ECCS, award #16-10833). S. C.,

M. Manceau and M. Matheron thank the financial support of European Union's Horizon 2020 research and innovation programme under grant agreement No 763989 (APOLO project). F. De R. and T. M. W. would like to acknowledge the support from the Engineering and Physical Sciences Research Council (EPSRC) through the SPECIFIC Innovation and Knowledge Centre (EP/N020863/1) and express their gratitude to the Welsh Government for their support of the Ser Solar programme. P. A. T. acknowledges financial support from Russian Science Foundation (project No. 19-73-30020). J.K. acknowledges the support by the Solar Photovoltaic Academic Research Consortium II (SPARC II) project, gratefully funded by WEFO. M.K.N. acknowledges financial support from Innosuisse project 25590.1 PFNM-NM, Solaronix, Aubonne, Switzerland. C.-Q. M. would like to acknowledge The Bureau of International Cooperation of Chinese Academy of Sciences for the support of ISOS11 and the Ministry of Science and Technology of China for the financial support (No 2016YFA0200700). N.G.P. acknowledges financial support from the National Research Foundation of Korea (NRF) grants funded by the Ministry of Science, ICT Future Planning (MSIP) of Korea under contracts NRF-2012M3A6A7054861 and NRF-2014M3A6A7060583 (Global Frontier R&D Program on Center for Multiscale Energy System). CSIRO's contribution to this work was conducted with funding support from the Australian Renewable Energy Agency (ARENA) through its Advancing Renewables Program. A. F. N gratefully acknowledges support from FAPESP (Grant 2017/11986-5) and Shell and the strategic importance of the support given by ANP (Brazil's National Oil, Natural Gas and Biofuels Agency) through the R&D levy regulation. Y.-L.L. and Q.B. acknowledge support from the National Science Foundation Division of Civil, Mechanical and Manufacturing Innovation under award #1824674. S.D.S. acknowledges the European Research Council (ERC) under the European Union's Horizon 2020 research and innovation programme (HYPERION, grant agreement No. 756962), and the Royal Society and Tata Group (UF150033). The work at the National Renewable Energy Laboratory was supported by the U.S. Department of Energy (DOE) under contract DE-AC36-08GO28308 with Alliance for Sustainable Energy LLC, the manager and operator of the National Renewable Energy Laboratory. The authors (J.J.B, J.M.L., M.O.R, K.Z.) acknowledge support from the De-risking halide perovskite solar cells program of the National Center for Photovoltaics, funded by the U.S. Department of Energy, Office of Energy Efficiency and Renewable Energy, Solar Energy Technology Office. The views expressed in the article do not necessarily represent the views of the DOE or the U.S. Government. The U.S.

Government retains and the publisher, by accepting the article for publication, acknowledges that the U.S. Government retains a nonexclusive, paid-up, irrevocable, worldwide license to publish or reproduce the published form of this work, or allow others to do so, for U.S. Government purposes. H.J.S. acknowledges the support of EPSRC UK, Engineering and Physical Sciences Research Council. V.T. and M. Madsen acknowledges 'Villum Foundation' for funding of the project CompliantPV, under project number 13365. M. Madsen acknowledges 'Danmarks Frie Forskningsfond, DFF FTP for funding of the project React-PV, No. 8022-00389B. M.G. and S.M.Z. thank the King Abdulaziz City for Science and technology (KACST) for financial support. M.L.C. and H.X. acknowledges the support from Spanish MINECO for the grant GraPErOs (ENE2016-79282-C5-2-R) and the OrgEnergy Excelence Network CTQ2016-81911-REDT and the Agència de Gestiód'Ajuts Universitaris i de Recerca for the support to the consolidated Catalonia research group 217 SGR 329 and the Xarxa de Referència en Materials Avançats per a l'Energia (Xarmae). ICN2 is supported by the Severo Ochoa program from Spanish MINECO (Grant No. SEV-2017-0706) and is funded by the CERCA Programme / Generalitat de Catalunya. S.V. acknowledges TKI-UE/Ministry of Economic Affairs for financial support of the TKI-UE toeslag project POP-ART (No. 1621103).

Author contributions

E.A.K. and M.L.-C. conceived the idea of the manuscript and organized a Round Table discussion of this issue at the 11th International Summit on Organic and Hybrid Photovoltaics Stability (ISOS 11). M.V.K. wrote the first draft. R.M. suggested the first version of the machine-readable template for stability data collection. All coauthors contributed to the writing of the paper.

Additional information

Supplementary information is available for this paper.

Correspondence and requests for materials should be addressed to E.A.K. and M.L.-C.

Competing interests

The authors declare no competing financial interests.

References

1. Best Research-Cell Efficiency Chart | Photovoltaic Research | NREL. Available at: https://www.nrel.gov/pv/cell-efficiency.html. (Accessed: 5th May 2019)
2. Green, M. A. *et al.* Solar cell efficiency tables (Version 53). *Prog. Photovolt. Res. Appl.* **27**, 3–12 (2019).
3. Lang Felix *et al.* Influence of Radiation on the Properties and the Stability of Hybrid Perovskites. *Adv. Mater.* **30**, 1702905 (2017).
4. Lee, S.-W. *et al.* UV Degradation and Recovery of Perovskite Solar Cells. *Sci. Rep.* **6**, srep38150 (2016).
5. Kim, N.-K. *et al.* Investigation of Thermally Induced Degradation in CH 3 NH 3 PbI 3 Perovskite Solar Cells using In-situ Synchrotron Radiation Analysis. *Sci. Rep.* **7**, 4645 (2017).
6. Schwenzer, J. A. *et al.* Temperature Variation Induced Performance Decline of Perovskite Solar Cells. *ACS Appl. Mater. Interfaces* **10**, 16390–16399 (2018).
7. Holzhey, P. *et al.* A chain is as strong as its weakest link – Stability study of MAPbI3 under light and temperature. *Mater. Today* (2018). doi:10.1016/j.mattod.2018.10.017
8. Yang, J., Siempelkamp, B. D., Liu, D. & Kelly, T. L. Investigation of CH3NH3PbI3 Degradation Rates and Mechanisms in Controlled Humidity Environments Using in Situ Techniques. *ACS Nano* **9**, 1955–1963 (2015).
9. Bryant, D. *et al.* Light and oxygen induced degradation limits the operational stability of methylammonium lead triiodide perovskite solar cells. *Energy Environ. Sci.* **9**, 1655–1660 (2016).
10. Howard, J. M. *et al.* Humidity-Induced Photoluminescence Hysteresis in Variable Cs/Br Ratio Hybrid Perovskites. *J. Phys. Chem. Lett.* **9**, 3463–3469 (2018).

11. Domanski, K., Alharbi, E. A., Hagfeldt, A., Grätzel, M. & Tress, W. Systematic investigation of the impact of operation conditions on the degradation behaviour of perovskite solar cells. *Nat. Energy* **3**, 61 (2018).
12. Khenkin, M. V., Anoop, K. M., Katz, E. & Visoly-Fisher, I. Bias-Dependent Degradation of Various Solar Cells: Lessons for Stability of Perovskite Photovoltaics. *Energy Environ. Sci.* **12**, 550–558 (2019).
13. Bae, S. *et al.* Electric-Field-Induced Degradation of Methylammonium Lead Iodide Perovskite Solar Cells. *J. Phys. Chem. Lett.* **7**, 3091–3096 (2016).
14. Reese, M. O. *et al.* Consensus stability testing protocols for organic photovoltaic materials and devices. *Sol. Energy Mater. Sol. Cells* **95**, 1253–1267 (2011).
15. Gevorgyan, S. A. *et al.* An inter-laboratory stability study of roll-to-roll coated flexible polymer solar modules. *Sol. Energy Mater. Sol. Cells* **95**, 1398–1416 (2011).
16. Madsen, M. V. *et al.* Worldwide outdoor round robin study of organic photovoltaic devices and modules. *Sol. Energy Mater. Sol. Cells* **130**, 281–290 (2014).
17. Tanenbaum, D. M. *et al.* The ISOS-3 inter-laboratory collaboration focused on the stability of a variety of organic photovoltaic devices. *RSC Adv.* **2**, 882–893 (2012).
18. Tiihonen, A. *et al.* Critical analysis on the quality of stability studies of perovskite and dye solar cells. *Energy Environ. Sci.* **11**, 730–738 (2018).
19. Boyd, C. C., Cheacharoen, R., Leijtens, T. & McGehee, M. D. Understanding Degradation Mechanisms and Improving Stability of Perovskite Photovoltaics. *Chem. Rev.* **119**, 3418–3451 (2018).
20. Abate, A., Correa-Baena, J.-P., Saliba, M., Su'ait, M. S. & Bella, F. Perovskite Solar Cells: From the Laboratory to the Assembly Line. *Chem. – Eur. J.* **24**, 3083–3100

21. Christians, J. A., Habisreutinger, S. N., Berry, J. J. & Luther, J. M. Stability in Perovskite Photovoltaics: A Paradigm for Newfangled Technologies. *ACS Energy Lett.* **3**, 2136–2143 (2018).
22. Saliba, M., Stolterfoht, M., Wolff, C. M., Neher, D. & Abate, A. Measuring Aging Stability of Perovskite Solar Cells. *Joule* **2**, 1019–1024 (2018).
23. Saliba, M. Perovskite solar cells must come of age. *Science* **359**, 388–389 (2018).
24. Yang, Y. & You, J. Make perovskite solar cells stable. *Nat. News* **544**, 155 (2017).
25. Snaith, H. J. & Hacke, P. Enabling reliability assessments of pre-commercial perovskite photovoltaics with lessons learned from industrial standards. *Nat. Energy* **3**, 459 (2018).
26. Meng, L., You, J. & Yang, Y. Addressing the stability issue of perovskite solar cells for commercial applications. *Nat. Commun.* **9**, 5265 (2018).
27. *Report on measurement and stability testing protocols*. (CHEOPS project, https://www.cheops-project.eu/uploads/7/0/9/9/70997359/cheops__653296__d2.1_measurementstabilitytestingprotocols_v1.pdf).
28. Dunbar, R. B. *et al.* How reliable are efficiency measurements of perovskite solar cells? The first inter-comparison, between two accredited and eight non-accredited laboratories. *J. Mater. Chem. A* **5**, 22542–22558 (2017).
29. Christians, J. A., Manser, J. S. & Kamat, P. V. Best Practices in Perovskite Solar Cell Efficiency Measurements. Avoiding the Error of Making Bad Cells Look Good. *J. Phys. Chem. Lett.* **6**, 852–857 (2015).
30. *IEC TR 63228 ED1 | Measurement protocols for photovoltaic devices based on organic, dye-sensitized or perovskite materials. International Electrotechnical Commission, Geneva*. (2019).
31. Howard, J. M., Tennyson, E. M., Neves, B. R. A. & Leite, M. S. Machine Learning for Perovskites' Reap-Rest-Recovery Cycle. *Joule* **3**, 325–337 (2018).

32. 11th International Summit on Organic and Hybrid Photovoltaic Stability: Home. Available at: http://isos11.csp.escience.cn/dct/page/1. (Accessed: 10th February 2019)
33. IEC 61215-1:2016 | IEC Webstore | rural electrification, solar power, solar panel, photovoltaic, PV, smart city, LVDC. Available at: https://webstore.iec.ch/publication/24312. (Accessed: 8th December 2018)
34. IEC 61215-1-2:2016 | IEC Webstore | rural electrification, solar power, solar panel, photovoltaic, PV, smart city, LVDC. Available at: https://webstore.iec.ch/publication/26860. (Accessed: 8th December 2018)
35. Tress, W. *et al.* Understanding the rate-dependent J–V hysteresis, slow time component, and aging in CH3NH3PbI3 perovskite solar cells: the role of a compensated electric field. *Energy Environ. Sci.* **8**, 995–1004 (2015).
36. L. Unger, E. *et al.* Hysteresis and transient behavior in current–voltage measurements of hybrid-perovskite absorber solar cells. *Energy Environ. Sci.* **7**, 3690–3698 (2014).
37. Jena, A. K., Kulkarni, A., Ikegami, M. & Miyasaka, T. Steady state performance, photo-induced performance degradation and their relation to transient hysteresis in perovskite solar cells. *J. Power Sources* **309**, 1–10 (2016).
38. Leguy, A. M. A. *et al.* Reversible Hydration of CH3NH3PbI3 in Films, Single Crystals, and Solar Cells. *Chem. Mater.* **27**, 3397–3407 (2015).
39. Noh, J. H., Im, S. H., Heo, J. H., Mandal, T. N. & Seok, S. I. Chemical Management for Colorful, Efficient, and Stable Inorganic–Organic Hybrid Nanostructured Solar Cells. *Nano Lett.* **13**, 1764–1769 (2013).
40. Lee, H., Lee, C. & Song, H.-J. Influence of Electrical Traps on the Current Density Degradation of Inverted Perovskite Solar Cells. *Mater. Basel Switz.* **12**, (2019).

41. Pearson, A. J. *et al.* Oxygen Degradation in Mesoporous Al2O3/CH3NH3PbI3-xClx Perovskite Solar Cells: Kinetics and Mechanisms. *Adv. Energy Mater.* **6**, 1600014

42. Anaya, M., Galisteo-López, J. F., Calvo, M. E., Espinós, J. P. & Míguez, H. Origin of Light-Induced Photophysical Effects in Organic Metal Halide Perovskites in the Presence of Oxygen. *J. Phys. Chem. Lett.* **9**, 3891–3896 (2018).

43. Haillant, O., Dumbleton, D. & Zielnik, A. An Arrhenius approach to estimating organic photovoltaic module weathering acceleration factors. *Sol. Energy Mater. Sol. Cells* **95**, 1889–1895 (2011).

44. Divitini, G. *et al. In situ* observation of heat-induced degradation of perovskite solar cells. *Nat. Energy* **1**, nenergy201512 (2016).

45. Abate, A. *et al.* Silolothiophene-linked triphenylamines as stable hole transporting materials for high efficiency perovskite solar cells. *Energy Environ. Sci.* **8**, 2946–2953 (2015).

46. Malinauskas, T. *et al.* Enhancing Thermal Stability and Lifetime of Solid-State Dye-Sensitized Solar Cells via Molecular Engineering of the Hole-Transporting Material Spiro-OMeTAD. *ACS Appl. Mater. Interfaces* **7**, 11107–11116 (2015).

47. Onoda-Yamamuro, N., Matsuo, T. & Suga, H. Calorimetric and IR spectroscopic studies of phase transitions in methylammonium trihalogenoplumbates (II)†. *J. Phys. Chem. Solids* **51**, 1383–1395 (1990).

48. Röhm, H. *et al.* Ferroelectric Properties of Perovskite Thin Films and Their Implications for Solar Energy Conversion. *Adv. Mater.* **0**, 1806661

49. Song, Z. *et al.* Perovskite Solar Cell Stability in Humid Air: Partially Reversible Phase Transitions in the PbI2-CH3NH3I-H2O System. *Adv. Energy Mater.* **6**, 1600846 (2016).

50. Osterwald, C. R. & McMahon, T. J. History of accelerated and qualification testing of terrestrial photovoltaic modules: A literature review. *Prog. Photovolt. Res. Appl.* **17**, 11–33 (2009).

51. Rosenthal, A. L., Thomas, M. G. & Durand, S. J. A ten year review of performance of photovoltaic systems. in *Conference Record of the Twenty Third IEEE Photovoltaic Specialists Conference - 1993 (Cat. No.93CH3283-9)* 1289–1291 (1993). doi:10.1109/PVSC.1993.346934

52. Kurtz, S. *et al.* A framework for a comparative accelerated testing standard for PV modules. in *2013 IEEE 39th Photovoltaic Specialists Conference (PVSC)* 0132–0138 (IEEE, 2013). doi:10.1109/PVSC.2013.6744114

53. Li, X. *et al.* Outdoor Performance and Stability under Elevated Temperatures and Long-Term Light Soaking of Triple-Layer Mesoporous Perovskite Photovoltaics. *Energy Technol.* **3**, 551–555 (2015).

54. Khenkin, M. V. *et al.* Reconsidering figures of merit for performance and stability of perovskite photovoltaics. *Energy Environ. Sci.* **11**, 739–743 (2018).

55. Reyna, Y. *et al.* Performance and stability of mixed FAPbI3(0.85)MAPbBr3(0.15) halide perovskite solar cells under outdoor conditions and the effect of low light irradiation. *Nano Energy* **30**, 570–579 (2016).

56. Stoichkov, V. *et al.* Outdoor performance monitoring of perovskite solar cell mini-modules: Diurnal performance, observance of reversible degradation and variation with climatic performance. *Sol. Energy* **170**, 549–556 (2018).

57. Tan, H. *et al.* Efficient and stable solution-processed planar perovskite solar cells via contact passivation. *Science* **355**, 722–726 (2017).

58. Christians, J. A. *et al.* Tailored interfaces of unencapsulated perovskite solar cells for >1,000 hour operational stability. *Nat. Energy* **3**, 68 (2018).

59. Gottesman, R. *et al.* Extremely Slow Photoconductivity Response of CH3NH3PbI3 Perovskites Suggesting Structural Changes under Working Conditions. *J. Phys. Chem. Lett.* **5**, 2662–2669 (2014).

60. Domanski, K. *et al.* Migration of cations induces reversible performance losses over day/night cycling in perovskite solar cells. *Energy Environ. Sci.* **10**, 604–613 (2017).

61. Cacovich, S. *et al.* Gold and iodine diffusion in large area perovskite solar cells under illumination. *Nanoscale* **9**, 4700–4706 (2017).

62. Deng, X. *et al.* Dynamic study of the light soaking effect on perovskite solar cells by in-situ photoluminescence microscopy. *Nano Energy* **46**, 356–364 (2018).

63. Duong, T. *et al.* Light and elevated temperature induced degradation (LeTID) in perovskite solar cells and development of stable semi-transparent cells. *Sol. Energy Mater. Sol. Cells* **188**, 27–36 (2018).

64. T. Hoke, E. *et al.* Reversible photo-induced trap formation in mixed-halide hybrid perovskites for photovoltaics. *Chem. Sci.* **6**, 613–617 (2015).

65. Duong, T. *et al.* Light and Electrically Induced Phase Segregation and Its Impact on the Stability of Quadruple Cation High Bandgap Perovskite Solar Cells. *ACS Appl. Mater. Interfaces* **9**, 26859–26866 (2017).

66. Ceratti, D. R. *et al.* Self-Healing Inside APbBr3 Halide Perovskite Crystals. *Adv. Mater.* **30**, 1706273

67. Nie, W. *et al.* Light-activated photocurrent degradation and self-healing in perovskite solar cells. *Nat. Commun.* **7**, ncomms11574 (2016).

68. Domanski, K. *et al.* Not All That Glitters Is Gold: Metal-Migration-Induced Degradation in Perovskite Solar Cells. *ACS Nano* **10**, 6306–6314 (2016).

69. Akbulatov, A. F. *et al.* Effect of Electron-Transport Material on Light-Induced Degradation of Inverted Planar Junction Perovskite Solar Cells. *Adv. Energy Mater.* **7**, 1700476 (2017).

70. Kettle, J. *et al.* Printable luminescent down shifter for enhancing efficiency and stability of organic photovoltaics. *Sol. Energy Mater. Sol. Cells* **144**, 481–487 (2016).

71. Gonzalez-Valls, I. & Lira-Cantu, M. Dye sensitized solar cells based on vertically-aligned ZnO nanorods: effect of UV light on power conversion efficiency and lifetime. *Energy Environ. Sci.* **3**, 789–795 (2010).

72. Melvin, A. A. *et al.* Lead iodide as a buffer layer in UV-induced degradation of CH3NH3PbI3 films. *Sol. Energy* **159**, 794–799 (2018).

73. Leijtens, T. *et al.* Overcoming ultraviolet light instability of sensitized TiO_2 with meso-superstructured organometal tri-halide perovskite solar cells. *Nat. Commun.* **4**, ncomms3885 (2013).

74. Shin, S. S. *et al.* Colloidally prepared La-doped BaSnO3 electrodes for efficient, photostable perovskite solar cells. *Science* **356**, 167–171 (2017).

75. Pérez-Tomas, A. *et al.* PbZrTiO 3 ferroelectric oxide as an electron extraction material for stable halide perovskite solar cells. *Sustain. Energy Fuels* **3**, 382–389 (2019).

76. Farooq, A. *et al.* Spectral Dependence of Degradation under Ultraviolet Light in Perovskite Solar Cells. *ACS Appl. Mater. Interfaces* **10**, 21985–21990 (2018).

77. Cheacharoen, R. *et al.* Design and understanding of encapsulated perovskite solar cells to withstand temperature cycling. *Energy Environ. Sci.* **11**, 144–150 (2018).

78. Holzhey, P. & Saliba, M. A full overview of international standards assessing the long-term stability of perovskite solar cells. *J. Mater. Chem. A* **6**, 21794–21808 (2018).

79. Tress, W. *et al.* Performance of perovskite solar cells under simulated temperature-illumination real-world operating conditions. *Nat. Energy* 1 (2019). doi:10.1038/s41560-019-0400-8

80. Bag, M. *et al.* Kinetics of Ion Transport in Perovskite Active Layers and Its Implications for Active Layer Stability. *J. Am. Chem. Soc.* **137**, 13130–13137 (2015).

81. Khenkin, M. V. *et al.* Dynamics of Photoinduced Degradation of Perovskite Photovoltaics: From Reversible to Irreversible Processes. *ACS Appl. Energy Mater.* **1**, 799–806 (2018).

82. Huang, F. *et al.* Fatigue behavior of planar CH3NH3PbI3 perovskite solar cells revealed by light on/off diurnal cycling. *Nano Energy* **27**, 509–514 (2016).

83. Jiang, L. *et al.* Fatigue stability of CH3NH3PbI3 based perovskite solar cells in day/night cycling. *Nano Energy* **58**, 687–694 (2019).

84. Zhao, C. *et al.* Perovskite Solar Cells: Revealing Underlying Processes Involved in Light Soaking Effects and Hysteresis Phenomena in Perovskite Solar Cells (Adv. Energy Mater. 14/2015). *Adv. Energy Mater.* **5**, 1500279 (2015).

85. Luchkin, S. Yu. *et al.* Reversible and Irreversible Electric Field Induced Morphological and Interfacial Transformations of Hybrid Lead Iodide Perovskites. *ACS Appl. Mater. Interfaces* **9**, 33478–33483 (2017).

86. Bowring Andrea R., Bertoluzzi Luca, O'Regan Brian C. & McGehee Michael D. Reverse Bias Behavior of Halide Perovskite Solar Cells. *Adv. Energy Mater.* **8**, 1702365 (2018).

87. Barbé, J. *et al.* Dark electrical bias effects on moisture-induced degradation in inverted lead halide perovskite solar cells measured by using advanced chemical probes. *Sustain. Energy Fuels* **2**, 905–914 (2018).

88. Leijtens, T. *et al.* Mapping Electric Field-Induced Switchable Poling and Structural Degradation in Hybrid Lead Halide Perovskite Thin Films. *Adv. Energy Mater.* **5**, 1500962 (2015).

89. Deng, X. *et al.* Electric field induced reversible and irreversible photoluminescence responses in methylammonium lead iodide perovskite. *J. Mater. Chem. C* **4**, 9060–9068 (2016).

90. Seyedmahmoudian, M. *et al.* Simulation and Hardware Implementation of New Maximum Power Point Tracking Technique for Partially Shaded PV System Using Hybrid DEPSO Method. *IEEE Trans. Sustain. Energy* **6**, 850–862 (2015).

91. Rajagopal, A., Williams, S. T., Chueh, C.-C. & Jen, A. K.-Y. Abnormal Current–Voltage Hysteresis Induced by Reverse Bias in Organic–Inorganic Hybrid Perovskite Photovoltaics. *J. Phys. Chem. Lett.* **7**, 995–1003 (2016).

92. Nisato, G. *et al.* Experimental comparison of high-performance water vapor permeation measurement methods. *Org. Electron.* **15**, 3746–3755 (2014).

93. Paetzold, R., Winnacker, A., Henseler, D., Cesari, V. & Heuser, K. Permeation rate measurements by electrical analysis of calcium corrosion. *Rev. Sci. Instrum.* **74**, 5147–5150 (2003).

94. Reese, M. O., Dameron, A. A. & Kempe, M. D. Quantitative calcium resistivity based method for accurate and scalable water vapor transmission rate measurement. *Rev. Sci. Instrum.* **82**, 085101 (2011).

95. Ultra-high barrier properties are finally measurable. Available at: https://www.encapsulation.fraunhofer.de/content/dam/fleet/de/documents/SEMPA/Datenblatt%20HiBarSens.pdf.

96. Klumbies, H., Müller-Meskamp, L., Mönch, T., Schubert, S. & Leo, K. The influence of laterally inhomogeneous corrosion on electrical and optical calcium moisture barrier characterization. *Rev. Sci. Instrum.* **84**, 024103 (2013).

97. Boldrighini, P. *et al.* Optical calcium test for measurement of multiple permeation pathways in flexible organic optoelectronic encapsulation. *Rev. Sci. Instrum.* **90**, 014710 (2019).

98. Uddin, A., Upama, M. B., Yi, H. & Duan, L. Encapsulation of Organic and Perovskite Solar Cells: A Review. *Coatings* **9**, 65 (2019).

99. Cheacharoen, R. *et al.* Encapsulating perovskite solar cells to withstand damp heat and thermal cycling. *Sustain. Energy Fuels* **2**, 2398–2406 (2018).

100. Li, B., Wang, M., Subair, R., Cao, G. & Tian, J. Significant Stability Enhancement of Perovskite Solar Cells by Facile Adhesive Encapsulation. *J. Phys. Chem. C* **122**, 25260–25267 (2018).

101. Matteocci, F. *et al.* Encapsulation for long-term stability enhancement of perovskite solar cells. *Nano Energy* **30**, 162–172 (2016).

102. Akbulatov, A. F. *et al.* Probing the Intrinsic Thermal and Photochemical Stability of Hybrid and Inorganic Lead Halide Perovskites. *J. Phys. Chem. Lett.* **8**, 1211–1218 (2017).

103. Conings, B. *et al.* Intrinsic Thermal Instability of Methylammonium Lead Trihalide Perovskite. *Adv. Energy Mater.* **5**, 1500477 (2015).

104. Yang, J. *et al.* Photostability of Perovskite Solar Cells: Unraveling Photostability of Mixed Cation Perovskite Films in Extreme Environment (Advanced Optical Materials 20/2018). *Adv. Opt. Mater.* **6**, 1870080 (2018).

105. Motti, S. G. *et al.* Photoinduced Emissive Trap States in Lead Halide Perovskite Semiconductors. *ACS Energy Lett.* **1**, 726–730 (2016).

106. A solar checklist. *Nat. Photonics* **9**, 703 (2015).

107. Czudek, A. *et al.* Transient Analysis during Maximum Power Point Tracking (TrAMPPT) to Assess Dynamic Response of Perovskite Solar Cells. *ArXiv190605028 Cond-Mat Physicsphysics* (2019).

108. C. Monokroussos *et al.* Accurate Power Measurements of High Capacitance PV Modules with Short Pulse Simulators in a Single Flash. *27th Eur. Photovolt. Sol. Energy Conf. Exhib.* 3687–3692 (2012). doi:10.4229/27thEUPVSEC2012-4BV.4.41

109. Pellet, N. *et al.* Hill climbing hysteresis of perovskite-based solar cells: a maximum power point tracking investigation. *Prog. Photovolt. Res. Appl.* **25**, 942–950 (2017).

110. Cimaroli, A. J. *et al.* Tracking the maximum power point of hysteretic perovskite solar cells using a predictive algorithm. *J. Mater. Chem. C* **5**, 10152–10157 (2017).

111. Bliss, M. *et al.* I-V performance characterisation of perovskite solar cells. *Photovolt. Sci. Appl. Technol. PVSAT-14* (2018).

112. Dusza, M., Strek, W. & Granek, F. Significance of light-soaking effect in proper analysis of degradation dynamics of organic solar cells. *J. Photonics Energy* **6**, 035503 (2016).

113. Emery, K. A. Solar simulators and I–V measurement methods. *Sol. Cells* **18**, 251–260 (1986).

114. Freitag, M. *et al.* Dye-sensitized solar cells for efficient power generation under ambient lighting. *Nat. Photonics* **11**, 372–378 (2017).

115. De Rossi, F., Pontecorvo, T. & Brown, T. M. Characterization of photovoltaic devices for indoor light harvesting and customization of flexible dye solar cells to deliver superior efficiency under artificial lighting. *Appl. Energy* **156**, 413–422 (2015).

116. Steim, R. *et al.* Organic photovoltaics for low light applications. *Sol. Energy Mater. Sol. Cells* **95**, 3256–3261 (2011).

117. Lee, H. K. H., Li, Z., Durrant, J. R. & Tsoi, W. C. Is organic photovoltaics promising for indoor applications? *Appl. Phys. Lett.* **108**, 253301 (2016).

118. Yang, S.-S., Hsieh, Z.-C., Keshtov, M. L., Sharma, G. D. & Chen, F.-C. Toward High-Performance Polymer Photovoltaic Devices for Low-Power Indoor Applications. *Sol. RRL* **1**, 1700174 (2017).

119. Lee, H. K. H. *et al.* Organic photovoltaic cells – promising indoor light harvesters for self-sustainable electronics. *J. Mater. Chem. A* **6**, 5618–5626 (2018).

120. Chen, C.-Y. *et al.* Perovskite Photovoltaics for Dim-Light Applications. *Adv. Funct. Mater.* **25**, 7064–7070 (2015).

121. Lucarelli, G., Di Giacomo, F., Zardetto, V., Creatore, M. & Brown, T. M. Efficient light harvesting from flexible perovskite solar cells under indoor white light-emitting diode illumination. *Nano Res.* **10**, 2130–2145 (2017).

122. ISO 8995-1:2002(en), Lighting of work places — Part 1: Indoor. Available at: https://www.iso.org/obp/ui/#iso:std:iso:8995:-1:ed-1:v1:en. (Accessed: 14th April 2019)

123. Minnaert, B. & Veelaert, P. A Proposal for Typical Artificial Light Sources for the Characterization of Indoor Photovoltaic Applications. *Energies* **7**, 1500–1516 (2014).

124. Li, Y., Grabham, N. J., Beeby, S. P. & Tudor, M. J. The effect of the type of illumination on the energy harvesting performance of solar cells. *Sol. Energy* **111**, 21–29 (2015).

125. Curtis, D. Predictions for the contribution of residential lighting to the carbon emissions of the UK to 2050. in *In EEDAL Conference* (2009).

126. Wang, Z. *et al.* Efficient and Air-Stable Mixed-Cation Lead Mixed-Halide Perovskite Solar Cells with n-Doped Organic Electron Extraction Layers. *Adv. Mater.* **29**, 1604186 (2017).

127. Roesch, R. *et al.* Procedures and Practices for Evaluating Thin-Film Solar Cell Stability. *Adv. Energy Mater.* **5**, 1501407 (2015).

128. Arora, N. *et al.* Perovskite solar cells with CuSCN hole extraction layers yield stabilized efficiencies greater than 20%. *Science* **358**, 768–771 (2017).

129. Saliba, M. *et al.* Cesium-containing triple cation perovskite solar cells: improved stability, reproducibility and high efficiency. *Energy Environ. Sci.* **9**, 1989–1997 (2016).

130. Bai, S. *et al.* Planar perovskite solar cells with long-term stability using ionic liquid additives. *Nature* **571**, 245 (2019).

131. Grancini, G. *et al.* One-Year stable perovskite solar cells by 2D/3D interface engineering. *Nat. Commun.* **8**, (2017).

132. Bush, K. A. *et al.* 23.6%-efficient monolithic perovskite/silicon tandem solar cells with improved stability. *Nat. Energy* **2**, 17009 (2017).

133. Kettle, J. *et al.* Using ISOS consensus test protocols for development of quantitative life test models in ageing of organic solar cells. *Sol. Energy Mater. Sol. Cells* **167**, 53–59 (2017).

134. Burlingame, Q. *et al.* Reliability of Small Molecule Organic Photovoltaics with Electron-Filtering Compound Buffer Layers. *Adv. Energy Mater.* **6**, 1601094 (2016).

135. Misra, R. K. *et al.* Effect of Halide Composition on the Photochemical Stability of Perovskite Photovoltaic Materials. *ChemSusChem* **9**, 2572–2577 (2016).

136. Tan, W. *et al.* Initial photochemical stability in perovskite solar cells based on the Cu electrode and the appropriate charge transport layers. *Synth. Met.* **246**, 101–107 (2018).

137. Wang, Z. *et al.* High irradiance performance of metal halide perovskites for concentrator photovoltaics. *Nat. Energy* **3**, 855–861 (2018).

138. Misra, R. K. *et al.* Temperature- and Component-Dependent Degradation of Perovskite Photovoltaic Materials under Concentrated Sunlight. *J. Phys. Chem. Lett.* **6**, 326–330 (2015).

139. Madsen, M. V., Tromholt, T., Norrman, K. & Krebs, F. C. Concentrated Light for Accelerated Photo Degradation of Polymer Materials. *Adv. Energy Mater.* **3**, 424–427 (2013).

140. Visoly-Fisher, I. *et al.* Concentrated sunlight for accelerated stability testing of organic photovoltaic materials: towards decoupling light intensity and temperature. *Sol. Energy Mater. Sol. Cells* **134**, 99–107 (2015).

141. Züfle, S., Hansson, R., Katz, E. A. & Moons, E. Initial photo-degradation of PCDTBT:PC70BM solar cells studied under various illumination conditions: Role of the hole transport layer. *Sol. Energy* **183**, 234–239 (2019).

142. Burlingame, Q. C. Operational Stability and Charge Transport in Fullerene-Based Organic Solar Cells. (The University of Michigan, 2018).

143. C. J. Brabec. *How to stabilize organic solar cells behind 100,000 hours of operational stability.* (2018).

144. Odabaşı, Ç. & Yıldırım, R. Performance analysis of perovskite solar cells in 2013–2018 using machine-learning tools. *Nano Energy* **56**, 770–791 (2019).

145. Saliba, M. Polyelemental, Multicomponent Perovskite Semiconductor Libraries through Combinatorial Screening. *Adv. Energy Mater.* **0**, 1803754